Paper: Jc17-4-6062

Tailor-Made Plate Design and Manufacturing System for Treating Bone Fractures in Small Animals

Akio Doi[*1], Hiroki Takahashi[*1], Bunei Syuto[*2], Masaaki Katayama[*3], Hiroyuki Nagashima[*4], and Masahiro Okumura[*5]

[*1]Advanced Visualization Laboratory, Iwate Prefectural University
152-52 Sugo, Takizawa-mura, Iwate-gun, Iwate 020-0173, Japan
E-mail: {doia, t-hiroki}@iwate-pu.ac.jp
[*2]Iwate University
3-18-3 Ueda, Morioka-shi, Iwate 020-8550, Japan
[*3]Animal Hospital, Iwate University
3-18-3 Ueda, Morioka-shi, Iwate 020-8550, Japan
[*4]Iwate Industrial Research Institute
2-4-25 Kitaiioka, Morioka-shi, Iwate 020-0857, Japan
[*5]Department of Veterinary Medicine, Hokkaido University
Kita 18, Nishi 9, Kita-ku, Sapporo, Hokkaido 060-0818, Japan
[Received 00/00/00; accepted 00/00/00]

We propose the use of a computer-aided design (CAD) system for treating bone fractures in small animals. During surgical planning, the veterinarian sketches a simple plate by referring to computed tomography images. A CAD operator then uses polygonal approximation (triangulation) of the surface of the bone region to model the plate. After the approximated shape is imported into the CAD system as a triangular mesh, a detailed design of the plate is prepared by referring to the abovementioned sketch. The plate can be designed to match the bone surface since the plate surface follows the curvature of the surface of the exported triangular mesh. The bone shape and the plate are eventually converted into polygons, and a structural model identical to the fractured part of the bone can be reproduced using a 3D printer, which allows for alignment to be performed at full scale. In this study, we examine the applicability of the proposed system by designing the most appropriately shaped plates for bone fracture therapy for small dogs brought to a veterinary clinic for treatment.

Keywords: tailor-made plate, 3D dimensional image, 3D CAD system, fracture, 3D printer

1. Introduction

At veterinary clinics, the treatment of fractures that require plating in small animals involves cutting a long flat plate to the necessary length and affixing it with appropriate screws while following the curvature of the bone surface (**Fig. 1**). The plate is made based on measurements taken from X-ray (computed radiography) and computed tomography (CT) images. However, the process of cutting

Fig. 1. A conventional plate affixed to a bone model.

and bending the plate either preoperatively or intraoperatively imposes a burden on veterinarians and requires considerable time. Furthermore, for nontrivial fracture sites (e.g., comminuted fractures), it is extremely difficult during surgery to prepare a plate that follows the bone shape.

Several approaches to tailor-made implants have been proposed [1–3]. The customized plate analysis using a finite element (FE) model for clavicle fractures was reported in [4, 5]. These primary disadvantages are the time and cost required for the design and manufacture of tailor-made plates. Therefore, we propose an economical and practical approach that delivers a tailor-made plate to customers, and the approach is suitable for the design and manufacture of tailor-made plates for treating fractures in small animals [6]. We utilize computer-aided design (CAD) with CT images taken preoperatively to design and manufacture appropriately-shaped plates for treating fractures. Initially, the veterinarian uses image processing to extract the region corresponding to the bone from the 3D image; then, a simple plate is designed by drawing a sketch while referring to the displayed image of the bone. A 3D-rendered image of the fracture site can be obtained from CT multi-slice images. The approximate values for the length and width of the plate, the number and locations of screw holes, and the curvature of the plate are estimated at this stage (**Fig. 2**). In **Fig. 2(A)**, the image on

(A) (B)

Fig. 2. (A) Example of a sketch prepared by a veterinarian using the proposed design system. (B) Front and side views of a manufactured plate.

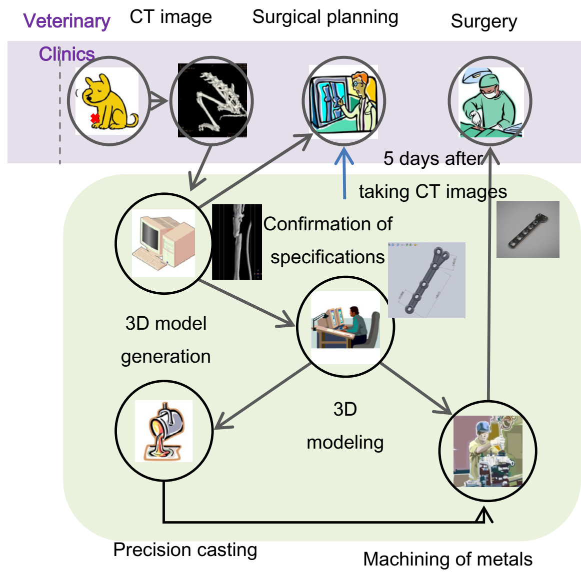

Fig. 3. Overall flow of the proposed design process.

the left shows the shape of the fractured bone, and the image on the right shows a sketch drawn on top of the mirror image of the corresponding bone on the unaffected side. **Fig. 2(B)** shows front and side views of the plate, together with the screw holes and the directions of the screws.

Based on this, a CAD operator models the plate using polygonal approximation (triangulation) of the surface of the bone region. After importing the approximated shape into the CAD system as a triangular mesh, a detailed design of the plate is prepared by referring to the above-mentioned sketch. Particularly in cases of simple bone fracture in a limb, the fracture site is extracted as separate partial images. These partial images are then joined by computer, and the restored bone shape is exported as a triangular mesh. As a result, the plate can be designed to match the bone surface since the plate surface follows the curvature of the surface of the exported triangular mesh. When the bone fracture is complex, however, mirror transformation of images of the corresponding bone on the unaffected side can be used because of the bilateral symmetry of the body. Then, after constructing the virtual bone shape, the plate can be designed to match it. In the proposed system, the bone shape and plate are eventually converted into polygons. A structural model identical to the fractured part of the bone can then be reproduced using a 3D printer, allowing for alignment to be performed at full scale. In this study, we examined the applicability of the proposed system by designing the most appropriately shaped plates for bone fracture therapy in small dogs brought to a veterinary clinic for treatment.

The remainder of this paper is structured as follows. Section 2 outlines the system structure and the design process, Section 3 describes multi-volume operations for 3D images, and Section 4 presents the process flow of generating tailor-made templates. Sections 5 and 6 covers the analysis and the manufacturing of the plates, respectively, and Section 7 presents the results of applying the system. Section 8 provides our concluding remarks.

2. Outline of System Construction and Design Process

Figure 3 shows the overall process flow in the proposed design system [6]. The obtained multi-slice CT images are provided in Digital Imaging and Communications in Medicine (DICOM) format, in which location information at the time of acquisition is saved in each slice image. A high-resolution 3D image can be obtained when the gap between slice images is sufficiently narrow.

The 3D image prepared from the multi-slice images is divided into bone regions and other regions by using the image processing technique of binarization. Since commercial CAD systems cannot manipulate 3D images directly, the binarized bone region is converted into an isosurface of the bone surface (triangular mesh) through isosurface processing. At this stage, the bone isosurface is not defined as a solid model with a strict 3D geometry. Since the isosurface is extracted from CT images of a biological object, if the shape is complex, it suffers from various deficiencies, irregularities, and partitioning (e.g., multiple insular regions). Data reduction and alignment are therefore needed to convert the isosurface into a CAD model.

In the proposed system, if the generated isosurface is simple and allows for straightforward conversion into a solid model, then such conversion is performed. However, if conversion of the entire object is expected to be time-consuming or difficult to perform, a surface (free curve) approximating the triangulated isosurface is prepared, and the plate is designed based on the resulting approximation surface.

When conversion into a solid model is possible, various geometric operations and computer simulations can be performed with a CAD system. For example, the simulation capabilities of computer-aided engineering (CAE) systems can be used when more detailed evaluations are necessary, such as determining the degree of conformance between the bone surface and the mounting surface of the plate or performing stress analysis. Furthermore, full-scale models of the designed plate and the fractured bone can be manufactured with a 3D printer using resin or gyp-

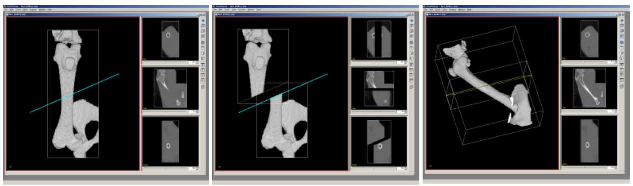

Fig. 4. Newly developed software tool for selecting cross-sectional planes, clipping 3D images, and connecting disjoint 3D images, respectively.

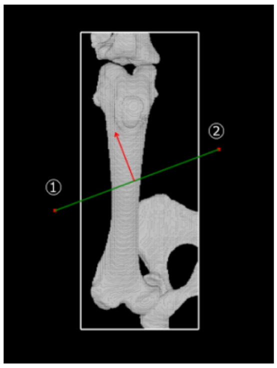

Fig. 5. Cutting plane (case A).

Fig. 6. Cutting plane (case B).

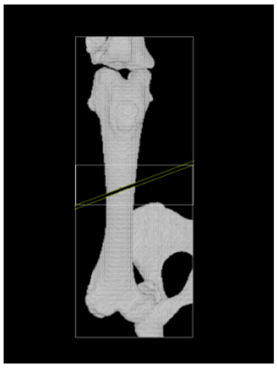

Fig. 7. Result of cutting.

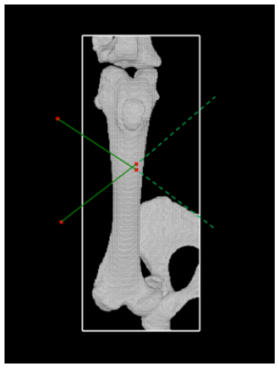

Fig. 8. Extended lines.

sum. This allows for final inspection of the shape, the screw hole locations, the conformance of the mounting surface with respect to the bone shape, and other parameters. The actual metal plate is prepared by molding, cutting, electron-beam melting, or other manufacturing method.

3. Multi-Volume Operations for 3D Images

3.1. Background and Objectives of Multi-Volume Operations

Conventional 3D image processing is used to manipulate individual 3D images. However, the advent of 64-bit operating systems, the constant improvement in central processing unit and graphics processor unit capabilities, and the increase in memory capacity of PCs have made it possible to manipulate multiple 3D images simultaneously on an ordinary personal computer. For example, the different modalities of CT and magnetic resonance imaging (MRI) are widely used in clinical medicine. We used a CT scanner to acquire slice images in the DICOM format before surgery. Several pieces of information, such as patient name, scan date, pixel resolution, pixel width, slice thickness, etc., are recorded in the DICOM image format. In particular, the world coordinates of slice position, slice thickness, and pixel resolution are important for 3D image construction. We have also developed a 3D image manipulation software tool for manipulating multiple images simultaneously.

3.2. Clipping 3D Image and Generating a Spliced Image with Cross-Section Alignment

The software tool for 3D image manipulation is referred to as JointVision in this paper. JointVision is capable of generating 3D images from slices; displaying, processing, and clipping 3D images; and splicing multiple 3D images. Each operation is performed interactively by the user while the 3D images are displayed (**Fig. 4**). JointVision is an OpenGL [7] application for Windows. A fast volume rendering system is also utilized, one that combines 3D texture compression and parallel programming techniques to render multiple high-resolution 3D images obtained with medical or industrial CT imaging [8–10]. If cross sections can be sufficiently approximated as planes, 3D images are cut along the cross-sectional planes, and a state close to that of the original healthy bone can be reproduced by connecting disjoint 3D images at cross-sectional planes. A software tool that interactively determines such cross-sectional planes and connects corresponding planes at clipping sites was developed in order to perform all of these operations.

3.3. Cut and Paste Operations Using Stroke

Although three side displays are commonly used for the manipulation of 3D objects in CAD, manipulation of 3D images remains a difficult and time-consuming task. Therefore, we propose a tablet-based method for visualizing 3D objects in JointVision. We utilize a directed line (referred to as a stroke) and define the cutting plane in 3D space on the display. The image is partitioned by the plane defined by the directed line. The line defines the direction of the normal to the cutting plane, and its orientation can be either positive or negative. Here, we show several examples of the proposed method in operation. The front and back surfaces of the cutting plane are defined by the orientation of the arrow (in the order of ①→②), as shown in **Figs. 5** and **6**. If there is only a single cutting plane, the result shown in **Fig. 7** will be the same regardless of the orientation of the front and back surfaces of the cutting plane. If the number of cutting planes is two or more, however, the results will change depending on the combination of orientations of front and back surfaces of each cutting plane. Also, the cutting plane is regarded as an extension on the display (dotted line in **Fig. 8**), and processing is performed by using the two cutting planes to divide the space into two regions, namely, the region en-

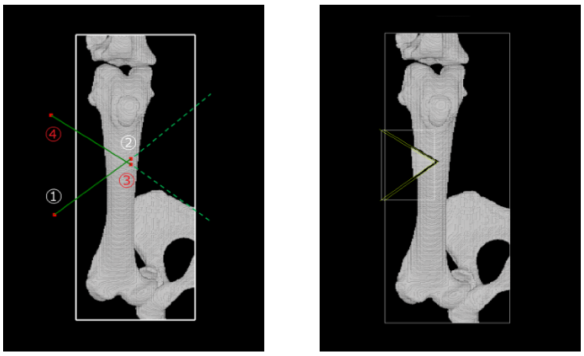

Fig. 9. Two cutting planes and the resulting cut region (case C).

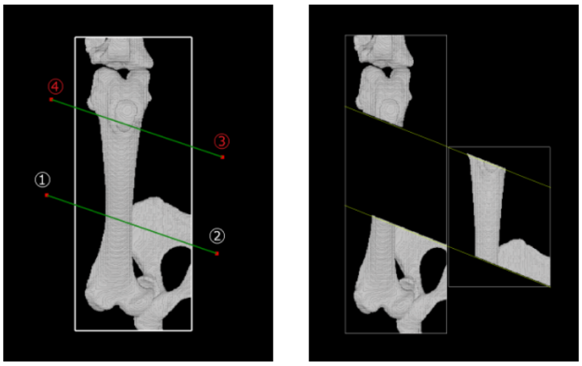

Fig. 10. Two cutting planes and the resulting cut region (case D).

closed by the front surfaces of the planes and the region corresponding to the remaining space. If there are two cutting planes, the direction of each segment in the stroke can be used to specify the area to be cut.

When two cutting planes are placed in the 3D image, the result depends on the orientation of the surface normal to the cutting plane. The two cases are shown in **Figs. 9** and **10**. Furthermore, the paste operation allows for the matching of two planes. For example, the surfaces of two cutting planes in the volume image are pasted together. This feature is used when two images need to be connected to each other with high precision. In our system, the user selects two surfaces interactively, and the first surface is repositioned onto the second one. After this, the volume image with the first surface can be moved and rotated horizontally onto the other surface (**Fig. 11**). In order to manipulate multiple volume images and graphics objects simultaneously, we utilize a volume rendering algorithm using 3D texture, and it is easy to implement the algorithm by using OpenGL.

4. Process Flow of Generating Tailor-Made Templates

4.1. Reproduction of Bone Surface Shape from CT Images

The acquired CT images are divided into bone regions (fractured and healthy bone) and other regions by binarization. The binarization threshold values are based on the Hounsfield units, which are between 300 and 500, and the values are configured interactively using a histogram as a reference. Since the threshold values differ in regions corresponding to cortical and cancellous bone tissue and cartilage, values corresponding to cortical bone tissue are selected in order to represent the entire bone surface. Automatic noise reduction and interactive cleaning are performed if small amounts of noise (salt-and-pepper noise), disjoint insular areas, artificial objects, or other irregularities are present after binarization.

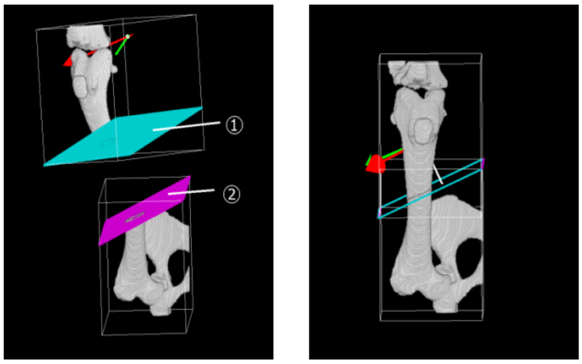

Fig. 11. Paste operation and its result.

4.2. Visualization of a Fractured Bone Through Mirror Transformation of its Healthy Counterpart

For complex fractures, when the original state of the bone is difficult to determine, an effective method involving horizontal flipping (mirror transformation) can be applied to the healthy bone on the unaffected side to construct a bone shape similar to the original shape of the fractured bone. Mirror transformation can be performed either in 3D image space or in 3D geometrical space in CAD. Here, we describe mirror transformation in 3D image space to illustrate the process of shaping the plate sought by the veterinarian in image space, which is more likely to be the method that would be used in veterinarian clinics. With respect to the transformed 3D image, after volume rendering and isosurface processing, an outline image (sketch) of the plate is drawn with the paint function on top of a screenshot of the image.

4.3. Reconstruction of Bone Surface Shape from Bone Surface Images

To construct a bone surface model (triangulation model) from the extracted bone region (3D image), the marching cubes method [11] is used to perform isosurface processing. Since a large amount of triangulation data is generated when applying isosurface processing to high-resolution CT images, data reduction processing is also performed using the quadric error method while preserving the surface shape characteristics [12]. A universal CAD system is used to record the generated triangulation

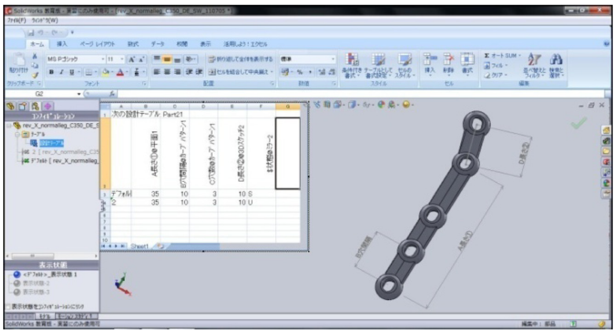

Fig. 12. Parameter table and generated plate in SolidWorks 2012.

model as a solid model. The CAD / computer-aided manufacturing / CAE systems used in this study were CATIA Version 5 (e.g., for analyzing the stress between the designed plate and bone surface) and SolidWorks 2012 by Dassault Systèmes.

4.4. Designing the Plate

To make the plate design as efficient as possible, a commonly used plate pattern is used at first, and the user inputs the necessary number of screw holes as a parameter. The plate type (standard shape) can be prepared according to user requirements. Although three types of patterns are currently available – a type with plain ends, a type where the angle of one end is changed, and a type with two screw holes at one end only – other plate types can be added as necessary (**Fig. 12**). Furthermore, the number of holes and their locations as well as the plate length, curvature, and other characteristics are parameterized for each plate type, and the user is provided with a form in which the parameters can be changed. The plate is regenerated automatically each time its parameters are altered. Thus, the process of designing the plate with the most appropriate shape for affixing to the bone surface is almost completely automated.

Figure 13 shows the surface regions on the repaired bone surface specified by the user through painting. **Fig. 14** shows B-spline surface generation on the bone surface, where an optimized tailor-made plate is designed by adjusting the curvature of the plate on the bone surface. Furthermore, **Fig. 15** shows an example of a tailor-made plate, and **Fig. 16** shows a cross-sectional image of the bone surface and the tailor-made plate.

Figure 17 shows another example for treating toe bone deformation in small dogs. In this case, we designed the plate interactively and considered the two bone surfaces. **Fig. 18** shows the design of the tailor-made plate, and **Fig. 19** shows the plate on the bone surfaces.

5. Analyzing Tailor-Made Plates

After designing the plate, the mechanical property values were input into the constructed finite element model (FEM). The boundary condition was applied, followed

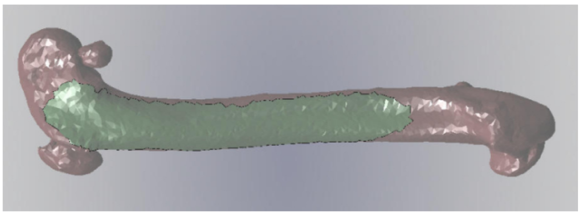

Fig. 13. Repaired bone and painted regions.

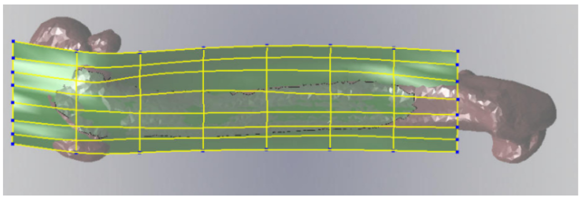

Fig. 14. Generation of bone surface through triangulation.

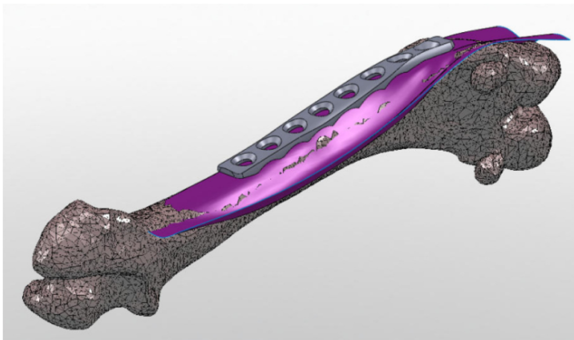

Fig. 15. Designing a tailor-made plate for the bone surface.

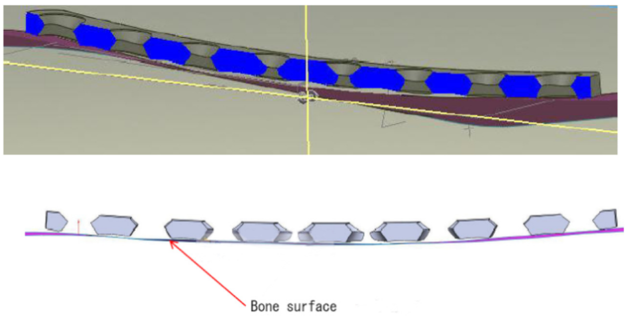

Fig. 16. Cross-sectional image of a tailor-made plate and the bone surface.

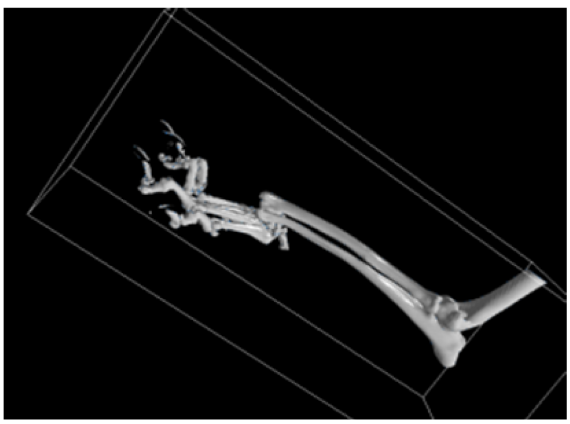

Fig. 17. CT image.

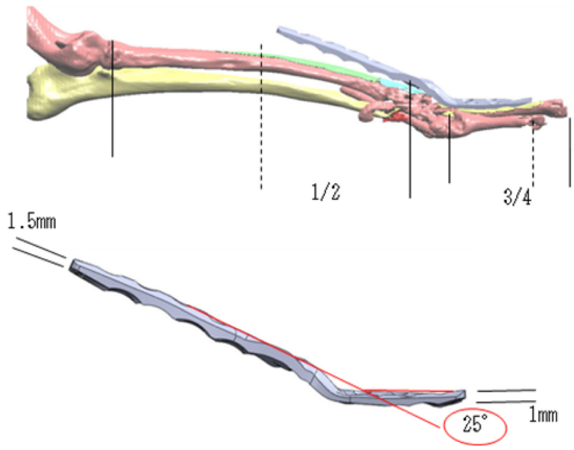

Fig. 18. A sketch document by a veterinarian.

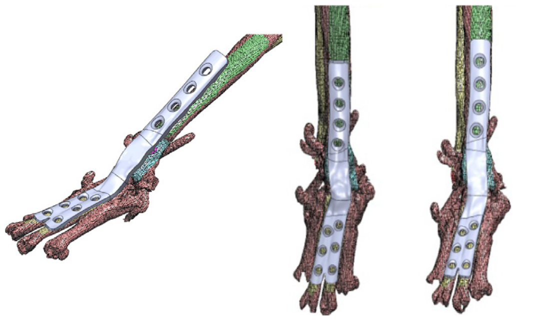

Fig. 19. The design of the tailor-made plate for the complicated bone surfaces.

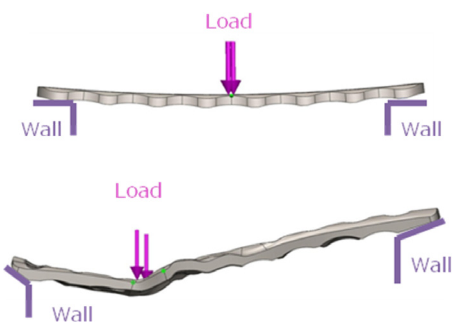

Fig. 20. Two boundary conditions.

by the calculation of an analysis solver of SolidWorks 2012. The analysis was a linear elastic stress analysis, and a 3D tetrahedron and pentahedron were employed. Our personal computer was a Dell Precision M6400 with 2.26 GHz Intel Core 2 Quad CPU, 7.98 GB RAM, and an Nvidia Quadro Fx 27000M graphics card.

Figure 20 shows the boundary condition of the analysis. The arrows pointing to the plate show the stress and the direction in which the strength of body weight and double body weight were applied; the bent lines at each end show the fixed walls. The friction type was Coulomb friction, and the friction coefficient μ was set at 0.001.

Through examination, we examined the cases, which are the strength of the load was equal to the body weight, 2 times the body weight, and 3 times the body weight. The material we used was Co-Cr-Mo alloy, the Young's ratio was 200 GPa, and the Poisson's ratio was 0.3.

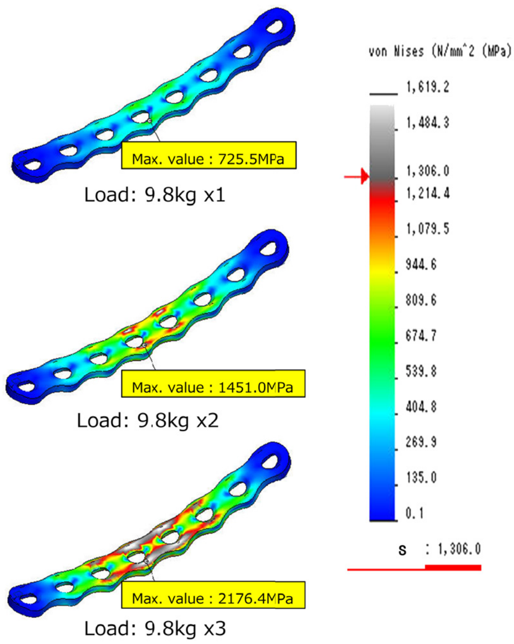

Fig. 21. The result of stress analysis (1).

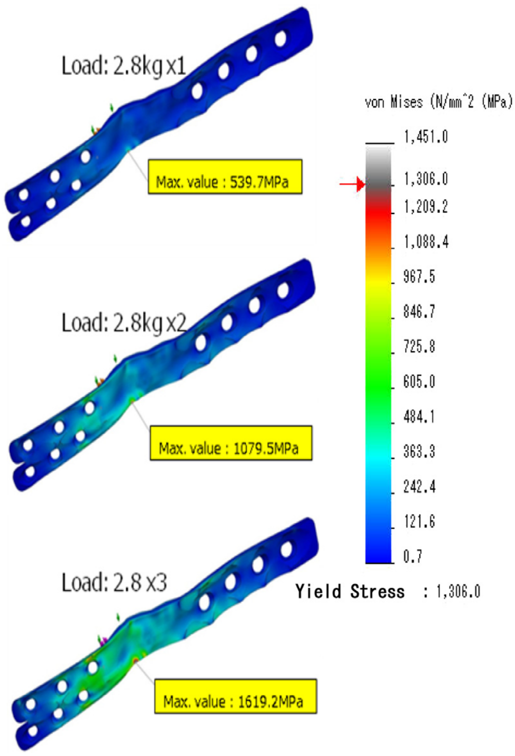

Fig. 22. The result of stress analysis (2).

Figure 21 shows the result of stress analysis in different loading conditions in the case of **Fig. 20** (upper). The body weight of the dog was 9.8 kg. A total of 9.8 kg, 19.6 kg, and 29.4 kg vertical loads were applied at the center position of the plate.

Figure 22 shows the result of stress analysis in different loading conditions in the case of **Fig. 20** (lower). The body weight of the dog was 2.8 kg. A total of 2.8 kg, 5.6 kg, and 8.4 kg vertical loads were applied at the weakest point of the plate. The total time to generate each mesh was about 3 minutes, and the computation time of the analysis was about 2 minutes.

In the case of **Fig. 21**, when the load was 19.6 kg, the maximum value came to 1451.0 MPa, and it was almost equal to the yield strength of the plate (1306.0 MPa). The safety factor was about 1.0.

In the case of **Fig. 22**, when the load was 8.4 kg, the maximum value came to 1619.2 MPa, 1.2 over for the yield strength (1306.0 MPa). The safety factor was over 0.8.

By using the stress analysis of the several conditions, we can estimate the optimized thickness of the plates and we can predict their weak points.

Fig. 23. Several tailor-made plate models manufactured with a 3D printer.

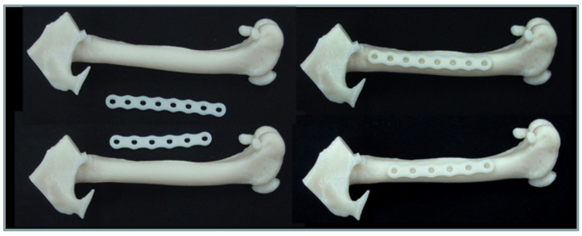

Fig. 24. Examples of structures manufactured to correspond to the bone shapes.

6. Manufacturing Tailor-Made Plates

After designing the plate, the materials, and the methods for processing and manufacturing, the actual plate and screws can be chosen from several options. Here we introduce samples manufactured by molding suitable materials, which include stainless steel, titanium alloy, and cobalt alloy.

In the example shown in **Fig. 8**, the most appropriate plate for the femur of a beagle used in the experiment was designed using CT images, after which a femur model and corresponding plate were manufactured with a 3D printer. In the upper and lower rows, the number of screw holes and the curvature in the vertical direction differed between individual dogs, and each plate was designed to match the surface of the corresponding bone. Since the extracted bone shape model is represented as a collection of triangles, a curved surface approximating this triangulated surface was prepared using the CAD system described above. The curvature of the resulting curved surface was subsequently used to design the plate. Gaps were left between the screw holes to ensure that blood flow was unobstructed. **Figs. 23** and **24** show examples of models of tailor-made plates and bones prepared with a 3D printer (Dimension SST 1200es; Stratasys, Inc.). The modeling material was acrylonitrile-butadiene-styrene resin, with a layer thickness of 0.254 mm (0.01 in). We utilized a vacuum-pressure casting machine (Heracast iQ; Heraeus, Ltd.) (**Fig. 25**), which performs high-quality reliable casting and is often used in dentistry. The metal used for casting the plate was a composite material composed of biomedical cobalt-chromium-molybdenum (Co-Cr-Mo) alloy [13, 14] with or without zirconium (Zr); the alloy was developed at the Institute for Materials Research Laboratory, Tohoku University. **Fig. 26** shows how the mold for casting was created.

Fig. 25. Vacuum-pressure casting machine.

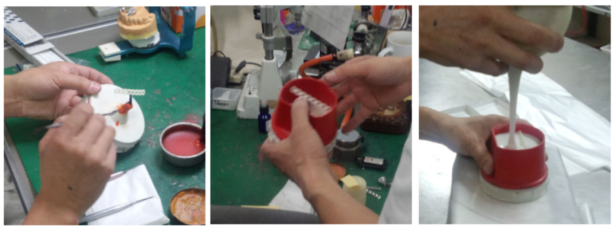

Fig. 26. Mold process of a tailor-made plate.

7. Results

The experimental animals were five dogs with bone fractures and one dog brought to the clinic for toe bone deformation treatment. **Table 1** shows the resolution and pitch size of CT images used in the evaluation. From CT images of the dogs, we generated isosurfaces of their femurs and designed six tailor-made plates in SolidWorks 2012. The process of designing the plates took around

Table 1. Resolution of CT images.

	Dog ID	Resolution [px]	Pitch [mm]
1	KQ5XJ	$512 \times 512 \times 1461$	(0.41, 0.41, 0.3)
2	TQ3XJ	$512 \times 512 \times 1351$	(0.368, 0.368, 0.3)
3	VQ5XJ	$512 \times 512 \times 1501$	(0.398, 0.398, 0.3)
4	FQ4XJ	$512 \times 512 \times 1401$	(0.337, 0.337, 0.3)
5	MQ5XJ	$512 \times 512 \times 1431$	(0.337, 0.337, 0.3)
6	REHA1	$512 \times 512 \times 491$	(0.117, 0.117, 0.3)

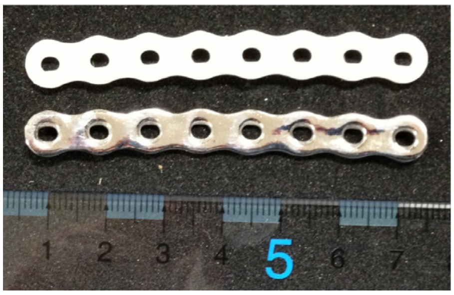

Fig. 27. Manufactured plates for affixing to the fractured bones of dogs in this study.

Fig. 28. Manufactured plates for affixing to the fractured bones of the respective dogs.

30 minutes for the five dogs with bone fracture and around 1 hour for the dog with toe bone deformation.

Using Co-Cr-Mo alloy, we made a total of 10 metal plates for the five dogs with bone fractures. Five plates were made with zirconium (Zr), and the other five plates were made without Zr.

Figures 27 and **28** show the plastic plate made by the 3D printer (upper) and the metal plate (lower) molded with the casting machine. Molding each plastic plate with a Dimension 3D printer (SST1200es, Stratasys, Inc., Waltham, MA) required about one hour. Casting and polishing each metal plate took two to three hours.

Figure 29 shows the overview of our design and manufacturing system for treating bone fractures in small animals.

Figures 30 and **31** show X-ray images of a Co-Cr-Mo alloy plate after surgery. The five plates with Zr and the five plates without Zr were affixed to the femurs of the five dogs with bone fractures to investigate the influence of the presence or absence of Zr on the adhesion of the plate to the bone surface.

The therapeutic plate of the dog brought to the clinic for toe bone deformation treatment was created using Co-Cr-Mo alloy with Zr. The opinion of the veterinary is that these plates are much easier to attach to bone surfaces than are the ordinary plates on the market.

The dog in **Fig. 31** has recovered and is walking. The bone is fixed, and there is no shift in the tailor-made plate on the deformed bone.

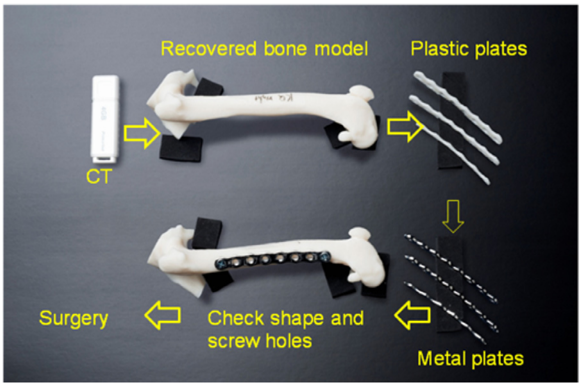

Fig. 29. Flow of design and manufacturing system.

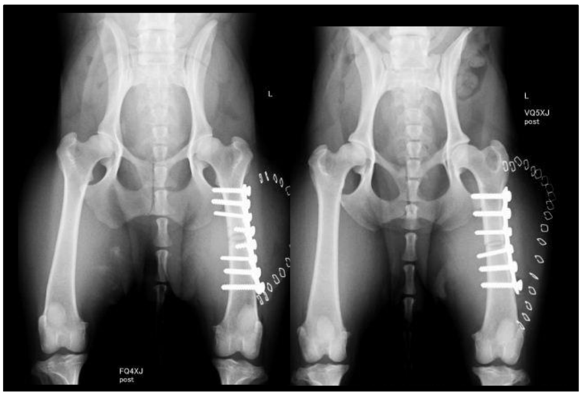

Fig. 30. X-ray images of the plates in **Fig. 27** after surgery.

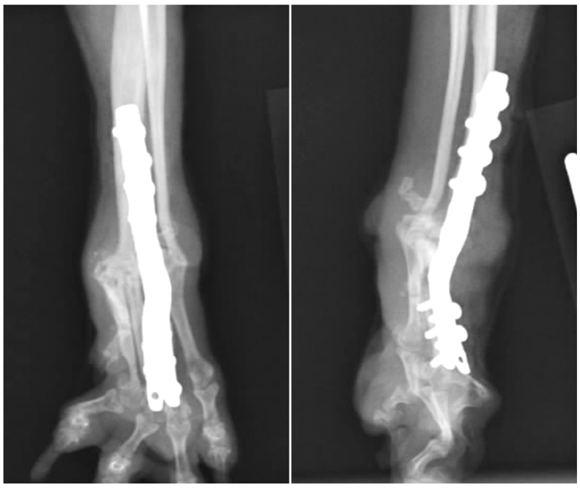

Fig. 31. Surgery results: plates affixed to the femurs of the respective dogs.

8. Conclusion

In contrast to conventional techniques, the proposed system allows the veterinarian to manufacture tailor-made plates preoperatively by referring to a sketch prepared from CT images. This drastically reduces the burden on the veterinarian during surgery. When the fracture is complex or the curvature of the mounting surface varies considerably, planar plates are rather difficult to cut and bend during surgery. Since tailor-made plates are designed, processed, and manufactured taking individual differences and the specifics of the particular case into account, the veterinarian can thus focus during surgery on affixing the plate to the fractured bone, reducing operating time. Furthermore, preoperative training and rigorous inspection can be conducted using bone models manufactured with 3D printers or similar technologies.

In the case of simple fractures, CT images are divided into partial images at the fractured bone surface, and the original state of the bone can be reproduced by moving and rotating each image. However, a method that has proved effective when the original state is difficult to determine due to the complexity of the fracture involves the horizontal flipping (mirror transformation) of images of the corresponding bone on the unaffected side and the preparation of a shape close to that of the original fractured bone. Mirror transformation also aids veterinarians in visualizing the shape of the healthy bone.

Although the most time-consuming part in the proposed approach is the manufacturing of the actual plate, small plates (up to 20 cm in length) can be molded within several hours by using highly precise molding techniques used in dentistry. Five-axis processing machines and cutting machines might be effective when larger plates are needed.

Acknowledgements

This research was supported in part by a Grant-in-Aid for Scientific Research (Project No.20500425) and the Regional Innovation Cluster Program under the Ministry of Education, Culture, Sports, Science, and Technology, Japan; the A-Step Research Fund of the Japan Science and Technology Agency; and the Iwate Prefectural University Academic Research Fund. This research was also supported in part by a Grant-in-Aid for the Strategic Information and Communications R&D Promotion Programme (SCOPE) under the Ministry of Internal Affairs and Communications. The authors thank Mr. Sachio Kurose, Mr. Masato Tamura, and Mr. Teruki Obara of the Iwate Digital Engineer Training Center for their support and help with designing the tailor-made plates.

References:

[1] O. Harrysson, Y. Hosni, and J. Nayfeh, "Custom-designed orthopedic implants evaluated using finite element analysis of patient-specific computed tomography data: femoral-component case study," BMC Musculoskelet Disorders, Vol.8, No.91, pp. 1-10, 2007.

[2] J. Davis and J. Bono, "Surgical strategies to achieve a custom-fit TKA with standard implant technique," J. of Orthopaedic, Vol.33, No.8, pp. 569-576, 2010.

[3] S. Choi, J. Lee, K. Igawa, O. Sugimoto, S. Suzuki, M. Mochizuki, R. Nishimura, U. Chung, and N. Sasaki, "Bone regeneration within a tailor-made tricalcium phosphate bone implant with both horizontal and vertical cylindrical holes transplanted into the skull of dogs," J. Artif Organs, Vol.12, No.4, pp. 274-277, 2009.

[4] D. Judd, M. Pallis, E. Smith, and C. Bottoni, "Acute Operative Stabilization Versus Nonoperative Management of Clavicle Fractures," The American Journal of Orthopedics, Vol.38, No.7, pp. 341-345. 2009.

[5] M. Cronskar and M. Backstrom, "Modeling of fractured clavicles and reconstruction plates using CAD, finite element analysis and real musculoskeletal forces input," WIT Press, BIOMED2013, pp. 235-243, 2013.

[6] A. Doi, H. Takahashi, B. Shuto, M. Katayama, H. Nagashima, and M. Okumura, "Design and application of tailor-made plates for treating fractures in small animals," IEEE iCAST 2012, 2012.

[7] "Open GL Programming Guide Fifth Edition – The Official Guide to Learning OpenGL, Version 2," Addison-Wesley Pearson Education, 2006.

[8] A. Doi, T. Takahashi, T. Mawatari, and S. Mega, "Development of a volume rendering system using 3D texture compression techniques on general-purpose personal computers," IEEE iCAST 2011, pp. 1-5, 2011.

[9] A. Doi, T. Takahashi, T. Mawatari, and S. Mega, "Development of Volume Rendering System Using 3D Texture Display Techniques and Its Applications," Medical Imaging Technology, Vol.30, No.2, pp. 83-91, 2012.

[10] AMD Corp., "3D (Volume) texturing and Volume Texture compression," ATI Radeon SDK Introduction Archive |AMD Developer Central, 2010.
http://developer.amd.com/gpu/radeon/archives/radeon_sdk_introduction

[11] W. Lorensen and H. Cline, "Marching cubes: A high resolution 3D surface construction algorithm," Computer Graphics, Vol.21, No.4, pp. 163-170, 1987.

[12] M. Garland and P. Heckbert, "Surface simplification using quadric error metrics," SIGGRAPH '97, pp. 209-216, 1997.

[13] E. Onodera, Y. Li, H. Matsumoto, and A. Chiba, "Intelligent hot forging process of artificial hip joint made of Ni-free Co-29Cr-6Mo-0.12N alloy," Steel Research International, Vol.81, pp. 362-365, 2010.

[14] S. Kurosu, H. Matsumoto, A. Chiba, C. Landron, D. Fabregue, and E. Maire, "The damage process in a biomedical Co-29Cr-6Mo-0.14N alloy analyzed by X-ray tomography and electron backscattered diffraction," SCRIPTA MATERIALIA, Vol.64, No.5, pp. 367-370, 2011.

Name:
Akio Doi

Affiliation:
Professor, Iwate Prefectural University

Address:
152-52 Sugo, Takizawa-mura, Iwate-gun, Iwate 020-0173, Japan

Brief Biographical History:

1984- Researcher, Tokyo Research Laboratory, IBM Japan Ltd.
1995- Associate Professor, Faculty of Engineering, Iwate University
1999- Professor, Faculty of Software and Information Science, Iwate Prefectural University

Main Works:

- medical imaging and scientific visualization

Membership in Academic Societies:

- The Visualization Society of Japan
- Information Processing Society of Japan (IPSJ)
- Association for Computing Machinery (ACM)

Name:
Hiroki Takahashi

Affiliation:
Researcher, Regional Community Cooperation Center, Iwate Prefectural University

Address:
152-89 Sugo, Takizawa-mura, Iwate-gun, Iwate 020-0173, Japan

Brief Biographical History:
2006 Graduated from Faculty of Software and Information Science, Iwate Prefuctural University
2008 Graduated from Master's Cource, Graduate of Software and Information Science, Iwate Prefuctural University
2008- Joined Netakiri-Hanbun Non-Profit Organization
2010- Guest Investigator, Community Cooperation Center, Iwate Prefectural University

Main Works:
• development of medical care system software

Name:
Masaaki Katayama

Affiliation:
Associate Professor of Small Animal Surgery, Cooperative Department of Veterinary Medicine, Faculty of Agriculture, Iwate University

Address:
3-18-8 Ueda, Morioka, Iwate 020-8550, Japan

Brief Biographical History:
2006- Assistant Professor, Department of Veterinary Medicine, Faculty of Agriculture, Iwate University
2012- Associate Professor, Cooperative Department of Veterinary Medicine, Faculty of Agriculture, Iwate University

Main Works:
• "Interaction of clarithromycin with cyclosporine in cats: pharmacokinetic study and case report," J. Feline. Med. Surg., Vol.14, pp. 257-261, 2012.

Membership in Academic Societies:
• Japanese Society of Transplantation
• Japanese Society of Veterinary Science

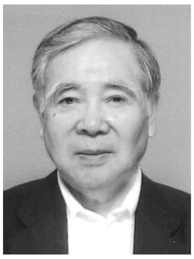

Name:
Bunei Syuto

Affiliation:
Visiting Professor, Iwate University

Address:
4-3-5 Ueda, Morioka, Iwate 020-8551, Japan

Brief Biographical History:
1991- Associate Professor, Faculty of Agriculture, Hokkaido University
1995- Professor, Faculty of Agriculture, Iwate University
2003- Visiting Professor, Iwate University

Main Works:
• biocompatibility evaluation of biomaterials

Membership in Academic Societies:
• The Japanese Society of Veterinary Science
• The Japan Institute of Metals and Material

Name:
Hiroyuki Nagashima

Affiliation:
Iwate Industrial Research Institute

Address:
2-4-25 Kitaiioka, Morioka, Iwate 020-0857, Japan

Brief Biographical History:
1998- Joined Iwate Industrial Research Institute

Membership in Academic Societies:
• The Japanese Society for the Science of Design (JSSD)
• The Japan Society of Kansei Engineering (JSKE)

Name:
Masahiro Okumura

Affiliation:
Professor, Graduate School of Veterinary Medicine, Hokkaido University

Address:
Kita 18, Nishi 9, Kita-ku, Sapporo, Hokkaido 060-0818, Japan

Brief Biographical History:
2003- Lecturer, Graduate School of Veterinary Medicine, Hokkaido University
2004- Associate Professor, Hokkaido University
2008- Professor, Hokkaido University
2012- Director, Lusaka Office, OIA, Hokkaido University

Main Works:
• Inhibitory effects of pentosan polysulfate sodium on MAP-kinase pathway and NF-κB nuclear translocation in canine chondrocytes in vitro

Membership in Academic Societies:
• Japanese Society of Veterinary Anesthesia and Surgery
• Japanese College of Small Animal Surgeons
• European Society of Veterinary Orthopedics and Traumatology